

Spectroscopic and Intermolecular Electron-Transfer Mechanism of Ferric (III) Ephedrine Complex as a Model of Drug Design

M.M. AL-Majthoub¹, Moamen S. Refat^{1,2,*}, Abdel Majid A. Adam¹ and M.A. Ahmed³

¹ Chemistry Department, Faculty of Science, Taif University, Al-Haweiah, P.O. Box 888, Zip Code 21974, Taif, Saudi Arabia

² Chemistry Department, Faculty of Science, Port Said University, Port Said, Egypt

³ Physics Chemistry, Faculty of Science, Al-Azhar University, Egypt

*E-mail: msrefat@yahoo.com

Received: 24 March 2013 / Accepted: 15 April 2013 / Published: 1 May 2013

A new ferric ephedrine complex, $[\text{Fe}(\text{eph})_2(\text{Cl})_2] \cdot \text{ClH}_2\text{O}$, was prepared. The chelating behavior of the ephedrine drug towards ferric(III) ions was discussed upon infrared, solid reflectance and Mössbauer spectroscopy. Ephedrine has two powerful donating sites –OH and –NH groups, so it is prefer to acts as bidentate ligand. The electronic spectra as well as the magnetic susceptibility measurements are speculate with each other the actual geometry. The Mössbauer spectral analysis are used as confirmatory tool for supporting the geometrical environment of Fe(III) complex. The thermal analysis TG/DTG/DSC is an important tool led to calculate the amount of solvent molecules inside or outside of coordination sphere also make follow-up for the stability of the prepared complex. The spectral and thermal analyses are supporting the coordination of the eph ligand in its neutral state. The Coats-Redfern relations were carried out to calculate the thermodynamic parameters for ferric complex.

Keywords: Ephedrine complex, Mössbauer, Thermal, Kinetics.

1. INTRODUCTION

Ephedra is a Phanerogame-Gymnosperme from the family of Gnetaceen. There are 30 different types of this plant-species known which grow in Asia, Mediterranean countries and America. Specially ephedra vulgaris, ephedra equisetina and ephedra sinica contain ephedrin with its other isomers. A certain ephedra species has been used in ancient Chinese medicine since ages. Already in 5000 B.C. an ephedra plant was widely used in China under the name Ma-Huang. Ma-Huang has been mentioned as medicine of moderate therapeutic range in the first Chinese pharmacopoe, published under the government of Shen Lung in 1760 B.C. A detailed description of the plant and its pharmacological

action is given in the Chinese pharmacopoe of modern times. The pharmacological studies have indicated that ephedrine is a sympathomimetic agonist at both α and β adrenergic receptors, which determine an increase of cardiac rate and contractility, peripheral vasoconstriction, bronchodilatation and central nervous system (CNS) stimulation [1]. Ephedrine is not the only alkaloid used in commercial products, since decongestant preparations usually contain pseudoephedrine. In recent years, the number of dietary supplements containing *Ephedra*, either as powdered botanical or, more frequently, as a standardized extract, had increased dramatically. Most of these products have been sold for the treatment of obesity or for increasing performance in body building. Often these dietary supplements also contained caffeine, either synthetic or from botanical extracts, in addition to other ingredients [2]. Weight loss and enhanced performance in body building may be due to the CNS stimulation and thermogenic properties of ephedrine [1]. However, severe contraindications have been given for individuals with hypertension or other cardiovascular diseases, glaucoma, diabetes and hyperthyroidism. Products containing *E. sinica* (or another botanical source of ephedrine) were among the most popular dietary supplements on the market, until their sale was banned by the U.S. Food and Drug Administration (FDA) in April 2004. After the ban of *Ephedra* products, “*Ephedra*-free” dietary supplements for weight loss were introduced. However, *Ephedra*-free is not necessarily danger-free [3]. *Citrus aurantium* is an ingredient in many of these *Ephedra*-free dietary supplements. The main active constituent of *C. aurantium* fruit extracts is (-)-synephrine [3], a phenethylamine alkaloid similar in structure to ephedrine. However, dietary supplements often contain *C. aurantium* in combination with concentrates of other herbs that are rich in caffeine and have the same potential to induce arrhythmia, hypertension, heart attacks and strokes as the combination of ephedrine and caffeine [3]. Depending on the oxidation state of metal, the coordination number and the kind of coordinated ligand, there are many structures, which show different biological and physico – chemical properties [4, 5]. The literature shows that there is a direct relationship between chemical structure and the antimicrobial properties of chemical compounds [6, 7]. Cui [6], for example, investigated a series of compounds containing NO groups and established that this group is exclusively responsible for the biological activity of some compounds. The author correlated the IR wave number of the valence vibration of the NO group with the antimicrobial activity of the compound. It was suggested that this parameter (the IR wave number) may be a good benchmark for determining the biological properties of compounds containing this group. Previously, the relationship between the chemical structure characterized by spectral parameters and antimicrobial activity was studied [5, 8, 9]. In this work, we prefer to throw a light on an essential compound as Ephedrine to evaluate the probability of its interaction with ferric(III) ions as a one of essential metals presented in the blood of human. This paper is considered the initial point for the specialists in the medicinal field for condensed investigation.

2. EXPERIMENTAL

2.1 Reagents

Ephedrine (2- (methylamino) – 1- phenylpropan – 1 –ol hydrochloride)(HMPH) used in this study was obtained from the Egyptian International Pharmaceutical Industrial Company (EIPICO). All

other chemicals used in the preparations were of analytical reagent grade, commercially available from different sources (Fluka Co. and Aldrich Co.). Ferric(III) metal salt used as ferric chloride(III) chloride hexahydrate. All solvents are used as it is without further purification.

2.2 Synthesis of the ephedrine ferric(III) complex

The ferric(III) complex was prepared by molar ratio 1 : 2 (1 mmol of $\text{FeCl}_3 \cdot 6\text{H}_2\text{O}$: 2 mmol eph) in water/ethanol (50/50 v/v) solution. The resulted mixture was heated under reflux for 3 hr. The complex was separated from the reaction mixture and washed with boiling ethanol and dried under vacuum over anhydrous CaCl_2 .

2.3 Instrumental analyses

Carbon and Hydrogen content was determined at the Microanalytical Unit of Cairo University. The analysis of metal ions and their conjugated anion (chloride) were carried out according to standard methods [10]. IR spectra were recorded on a Genesis II FT – IR spectrophotometer (KBr – discs) in the $\nu = 400 - 4000 \text{ cm}^{-1}$ range. Solid reflectance spectrum of ferric(III) eph complex was measured on UV-3101 PC, Shimadzu, UV-Vis. NIR Scanning Spectrophotometer. Magnetic data were calculated using Magnetic Susceptibility Balance, Sherwood Scientific, Cambridge Science Park Cambridge, England, at Temp 25°C in Cairo University. The molar conductivities of freshly prepared $1.0 \times 10^{-3} \text{ mol/cm}^3$ DMF solutions were measured for the soluble complex and eph free ligand using Jenway 4010 conductivity meter. The Mössbauer spectrum of the ferric(III)ephedrine complex sample was obtained at RT using standard constant acceleration spectrometer (Wiesel Spectrometer, German) in the transmission mode. The spectrum was accumulated for a base line count greater than $10^6/\text{channel}$. The $^{57}\text{Co}/\text{Rh}$. source is remaining at RT. α Fe foil was used to calibrate the Mössbauer derive and to calculate the isomer shift. The resulting spectrum was fitted to one doublet with Lorentzian line profile and the two absorption lines were assumed to have symmetric intensities and widths. TG/DTG/DSC measurements are made in an N_2 atmosphere between room temperature and 800°C using SCINCO DSC 1500 STA at Taif University.

3. RESULTS AND DISCUSSION

The carbon, hydrogen and nitrogen contents of brown ferric(III) ephedrine complex were performed and gave good agreement with calculated data. Yield: 66 %; m.p. $> 200^\circ\text{C}$. calcd. Found; For $\text{C}_{20}\text{H}_{34}\text{Cl}_5\text{FeN}_2\text{O}_3$ (MW = 583.61 g/mol): calcd.: C, 41.16; H, 5.87; N, 4.80; Cl, 30.37 %. Found: C, 41.06; H, 5.73; N, 4.67; Cl, 30.21%. The molar conductance value of ferric(III) ephedrine complex in DMF ($1.0 \times 10^{-3} \text{ mol/cm}^3$) was measured at room temperature and the value is equal $60 \text{ ohm}^{-1} \text{ cm}^2 \text{ mol}^{-1}$. The comparison between the value of ephedrine free ligand and its ferric(III) complex led us to concluded that ferric(III) complex has a slightly electrolyte, this meaning that one of chlorine atom exhibited in the out-sphere of coordination frame.

3.1 Infrared spectra

Table 1. Assignments of the IR essential spectral bands (cm^{-1}) of ephedrine and its ferric(III) complex

Compound	ν_{OH}	ν_{NH}	δ_{OH} (out of plane)	$\nu_{\text{C-O}}$	δ_{OH} (in plane)	δ_{NH}	$\nu_{\text{M-Cl}}$	$\nu_{\text{M-N}}$	$\nu_{\text{M-O}}$
Ephedrine	3330	2972	751	1051	1395	1591	---	---	---
Ferric(III) ephedrine	3327	3139	755	1047	1402	1596	---	446	520

A deliberate comparison between the significant band positions in between the ephedrine HCl free ligand with its relative ferric(III) complex may give enough insight to elucidate the way of bonding of eph ligand towards the ferric(III) ion. Especially, with the absence of powerful technique such as X – ray crystallography. All spectra were carried in the range of $4000 - 400 \text{ cm}^{-1}$ and the most significant bands are listed in Table 1. The spectrum of free ligand displays a series of significant bands as: 3330, 2972, 1591 and 1395 cm^{-1} which may assign to $\nu(\text{OH})$, $\nu(\text{NH})$, $\delta(\text{NH})$ and $\delta(\text{OH})$ - in plane bend. The lower appearance shinned on bands of OH and NH groups supports of the presence of intraligand H – bonding (Fig. 1) between the two neighboring groups. Ephedrine ligand bonded towards ferric(III) ion by mode of coordination through its two active (– OH and – NH) sites in neutral state. This is expected due to the distribution of OH and NH groups, which primates this behavior as appeared from molecular modeling for the minimum internal energy structure (3.385 kcal/mol) by the use of MM^+ [11] force – field as implemented in hyperchem 5.1 [12]. The ν and δ OH in ferric(III) complex are more or less unshifted which may support its interaction after the decomposition of intraligand H – bonding. According to elemental analysis and thermogravimetric studies, the ferric(III) complex resulted contain one water molecules as crystallization [13]. The new bands assigned for $\nu(\text{M-N})$ and $\nu(\text{M-O})$ are easily characterized in the low frequency field except $\nu(\text{M-Cl})$ which cannot detected in the scanning range.

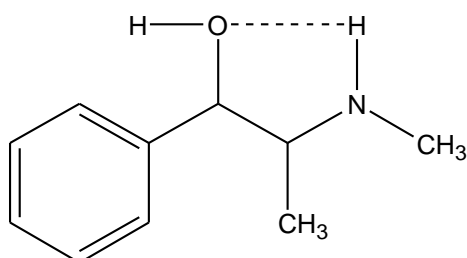


Figure 1. The modeling structure of ephedrine.

3.2 Magnetic susceptibility and solid reflectance spectral measurements

The diffuse solid reflectance spectrum of the Fe(III) ephedrine complex shows absorption bands at 16393 and 17699 cm^{-1} . The first band may be assigned to ${}^6\text{A}_1 \rightarrow 4\text{A}_1$, ${}^4\text{E}(\text{G})$, transition, while the

second band would be due to ${}^6A_1 \rightarrow {}^4T_2(G)$ transition, suggesting an octahedral arrangement around the Fe(III) ion [14]. The magnetic moment value μ_{eff} , (5.59 B.M.) is in the range of the octahedral geometries. The proposed structure of the ferric(III) ephedrine complex is shown in Fig. 2.

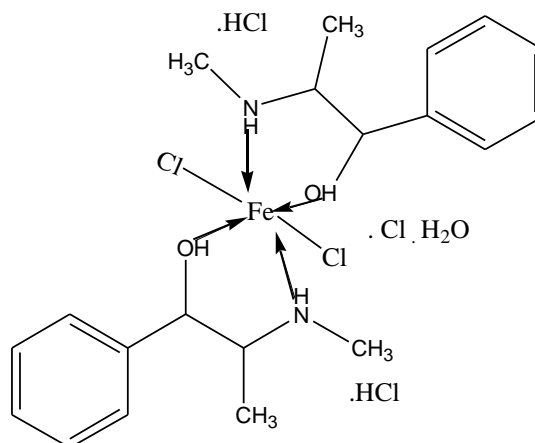


Figure 2. Suggested structure of ferric (III) ephedrine complex $[\text{Fe}(\text{eph})_2(\text{Cl})_2] \cdot \text{ClH}_2\text{O}$.

3.3 Mössbauer spectral Analysis

Table 2. Mössbauer Data of ferric (III) ephedrine complex at room temperature.

Compound	* δ_{Fe} mm/s	ΔE_Q mm/s	Γ mm/s	Assignment
$[\text{Fe}(\text{eph})_2(\text{Cl})_2] \cdot \text{ClH}_2\text{O}$	0.37	0.625	0.48	${}^{\text{IV}}\text{Fe}$ site

* δ_{Fe} is relative to α iron at room temperature

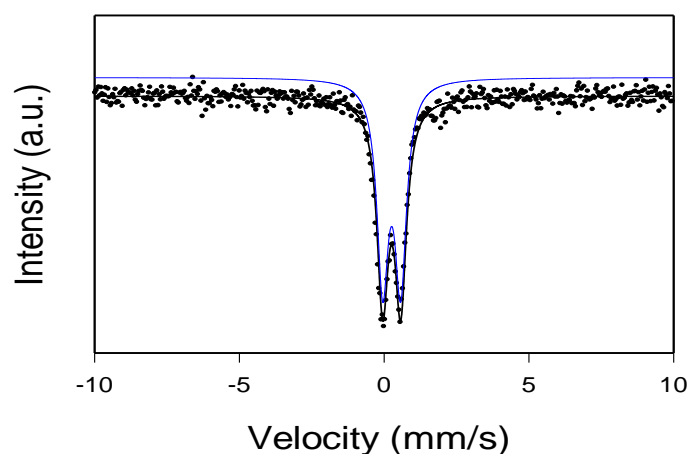


Figure 3. Mössbauer spectrum of ferric ephedrine complex at room temperature.

Figure 3 shows the room temperature Mössbauer spectrum of the ferric (III) ephedrine complex. In order to identify the coordination site of the iron in the complex, the Mossbauer parameters is reported in Table 2. Obviously the spectrum showing one para magnetic doublet whose

Mössbauer parameters corresponding to ferric (III) ions occupying the octahedral site [15]. This result was supported the suggested structure of ferric (III) ephedrine complex: $[\text{Fe}(\text{eph})_2(\text{Cl})_2] \cdot \text{ClH}_2\text{O}$, shown in Fig.2.

3.4 Thermal analyses (TG/DTG/DSC) studies

Simultaneous TG/DTG curves of $[\text{Fe}(\text{eph})_2(\text{Cl})_2] \cdot \text{ClH}_2\text{O}$ complex are shown in Fig. 4. The first mass loss (3.08%) between 30-120 °C corresponding to the endothermic peak below 100 °C is due to dehydration. The second and third mass losses occurred from 120-to-230 °C (4.42%) and from 230-to-300 °C (12.00%); the first of these occurred at $T_{\text{max}} = 235$ °C due to losses of two methyl groups and the second mass losses at $T_{\text{max}} = 295$ °C assigned to the loss of two hydrochloric acid molecules. There are four overlapping steps at 370, 430, 510 and 600 °C, for mass losses, the corresponding exothermic and endothermic peaks were attributed to the thermal decomposition of the ephedrine ligand. The thermal calculations based on the mass loss up to the final temperature are in agreement with the formation of iron metal as the final residual. An exothermic peak seen between starting temperature and 120 °C having its maximum at 75 °C, which show a low value attributed to the transition phase of the anhydrous $[\text{Fe}(\text{eph})_2(\text{Cl})_2] \cdot \text{Cl}$ complex. Fig. 4, show the DSC curve for ferric(III) complex in nitrogen atmosphere at heating rate 5 °C min^{-1} . The DSC exothermic events at 75, 235, 295, 370, 430 and 600 °C but only one endothermic peak at 510 °C corresponding to dehydration and decomposition of both ephedrine hydrochloride ligand molecules.

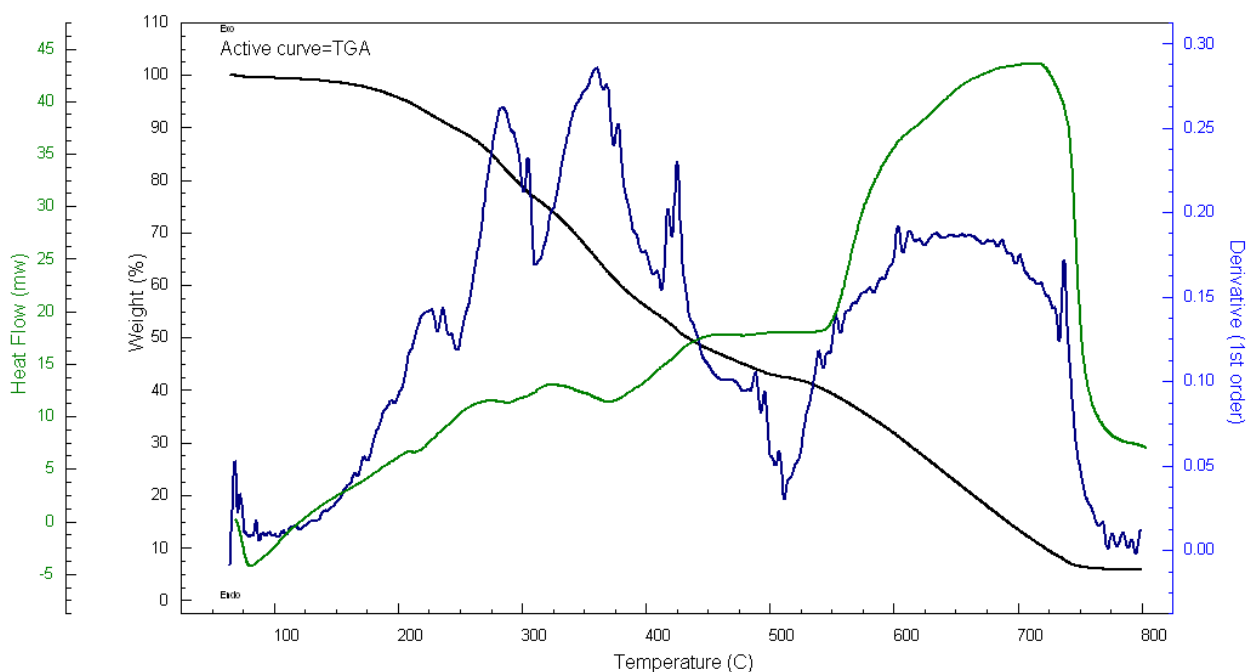


Figure 4. TG/DTG/DSC curves of ferric (III) ephedrine complex.

3.5 Kinetic thermodynamic parameters

Table 3. Kinetic parameters using the Coats – Redfern (CR) operated for the ferric(III) ephedrine complex at different decomposition steps.

Step	Kinetic Parameters					
	E (Jmol ⁻¹)	A (S ⁻¹)	Δ S (Jmol ⁻¹ K ⁻¹)	Δ H (Jmol ⁻¹)	Δ G (Jmol ⁻¹)	r
75 °C	1.40E+05	2.97E+17	8.83E+01	1.37E+05	1.065E+05	0.9901
235 °C	7.93E+04	2.96E+06	-1.25E+02	7.50E+04	1.39E+05	0.9889
295 °C	2.07E+05	2.38E+17	8.24E+01	2.02E+05	1.55E+05	0.9942
370 °C	1.62E+05	2.00E+11	-3.50E+01	1.70E+05	1.79E+05	0.9997
430 °C	3.01E+05	2.96E+20	1.40E+02	2.95E+05	1.97E+05	0.9909
510 °C	8.86E+04	4.875+03	-1.82E+02	8.21E+04	2.25E+05	0.9967
600 °C	1.52E+05	1.57E+06	-1.35E+02	1.44E+05	2.62E+05	0.9976

The kinetic parameters (Table 3) such as activation energy (ΔE^*), enthalpy of activation (ΔH^*), entropy of activation (ΔS^*), free energy change of decomposition (ΔG^*) were evaluated graphically by employing the Coats – Redfern relation [16] (Fig. 5) for investigated ferric(III) ephedrine complex. The equation is a typical integral method, represented as:

$$\int_0^{\alpha} \frac{d\alpha}{(1-\alpha)^n} = \frac{A}{\phi} \int_{T_1}^{T_2} \exp\left(\frac{-E^*}{RT}\right) dt$$

For convenience of integration the lower limit T_1 is usually taken as zero. This equation on integration gives:

$$\ln\left[\frac{-\ln(1-\alpha)}{T^2}\right] = \ln\left(\frac{AR}{\phi E^*}\right) - \frac{E^*}{RT}$$

A plot of $\ln\left[\frac{-\ln(1-\alpha)}{T^2}\right]$ (LHS) against $1/T$ was drawn. E^* is the energy of activation in Jmol⁻¹

and calculated from the slop and A is (S⁻¹) from the intercept value. The entropy of activation ΔS^* in (J K⁻¹mol⁻¹) was calculated by using the equation:

$$\Delta S^* = R \ln\left(\frac{Ah}{k_B T_s}\right)$$

Where k_B is the Boltzmann constant, h is the Plank's constant and T_s is the DTG peak temperature. All decomposition steps of ferric(III) complex was discussed which have negative entropy, which indicates that the complexes are formed spontaneously. The negative entropy also

indicates a more ordered activated state that may be possible through the chemisorptions of oxygen and other decomposition products. The negative values of the entropies of activation are compensated by the values of the enthalpies of activation, leading to almost the same values for the free energies of activation [17]. A positive change in entropy of activation at first, third and fifth steps indicate that the system has become more disordered. Degrees of freedom are “liberated” on going from the ground state to the transition state.

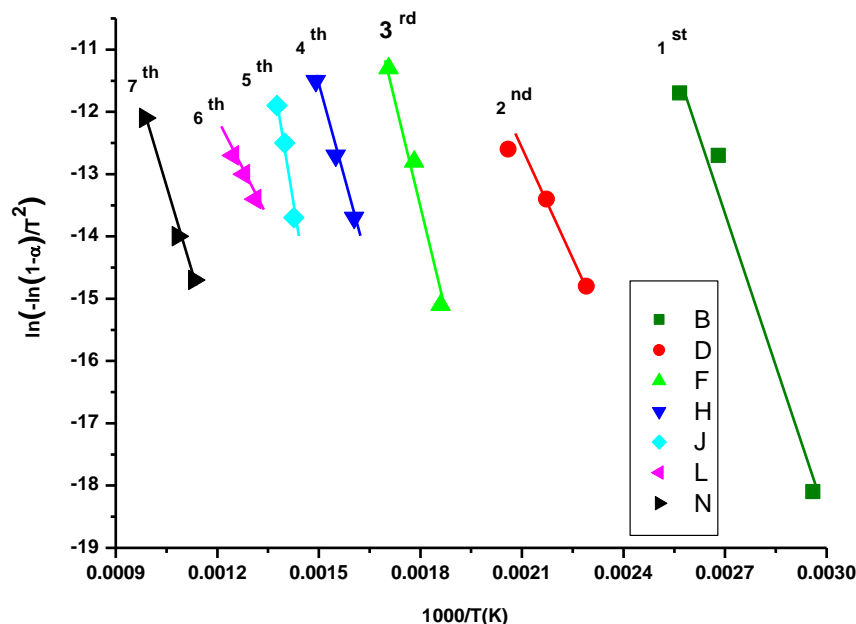


Figure 5. Coats–Redfern curves of ferric (III) ephedrine complex at different decomposition steps 1st (B), 2nd (D), 3rd (F), 4th (H), 5th (J), 6th (L) and 7th (N), respectively.

Electrochemical aspects in this research are to take advantage of the three analytical devices used namely molar conductivities, Mössbauer spectroscopy and solid reflectance. Upon the data of molar conductivities in comparison between free ephedrine free ligand and ferric (III) ephedrine complex these assigned to presence of one ionisable chloride ion outside of coordination sphere. Also, Mössbauer spectroscopy is unique in its sensitivity to subtle changes in the chemical environment of the nucleus including oxidation state changes, the effect of different ligands on a particular atom, and the magnetic environment of the sample. As an analytical tool Mössbauer spectroscopy offers detection limits in the order of billionths of an electron volt [18]. It has been especially useful in the field for identification the composition of iron-containing specimens. Mössbauer spectroscopy is mainly used for the characterization of electrode materials and the analysis of electrochemical reactions [19].

References

1. B.T. Schaneberg, S. Crockett, E. Badir, I.A. Khan. *Photochemistry* 62 (2003) 911.
2. M.C. Roman. *J. AOAC Int.* 87 (2004) 1.

3. F. Pellati, S. Benvenuti. *J. Chromatogr. A* 1161 (2007) 71.
4. R. L. Lieberman, A. Bino, N. Mirsky, D. A. Summers, R. C. Thompson. *Inorg. Chim. Acta* 297 (2000) 1.
5. P. koczoń, J. Piekut, M. Borawska, W. Lewandowski. *J. Mol. Struct.* 651 (2003) 67.
6. X. Cui, C. Joannou, M. Hughes, R. Cammack. *FEMS Microbiol. Lett.* 98 (1998) 67.
7. F. Hueso- Urena, M. Moreno – carretero, M. Romero – Molina, J. Salas – Peregrin, M. Sanchez – Sanchez, G. Alvarez de Cienfuegos – Lopez, R. Faure. *J. Inorg. Biochem.* 51 (1993) 613.
8. P. Koczoń, J. Piekut, M. Borawska, R. Świslocka, W. Lewandowski. *Spectrochim. Acta A* 61 (2005) 1917.
9. P. koczoń, J. Piekut, M. Borawska, R. Świslocka, W. Lewandowski. *Anal. Biochem.* 302 (2005) 302.
10. A. I. Vogel, A Text Book of Quantitative Inorganic Analysis, Longman, London (1994).
11. N. L. Allinger. *J. Am. Chem. Soc.* 99 (1977) 8127.
12. Hyper chem. Version 7.51 Hyper cube, INC.
13. Z. M. Zaki, G. G. Mohamed. *Spectrochim. Acta A* 56 (2000) 1245.
14. J.C. Bailar, H. Emeleus, J.R. Nyholm, A.F. Dickenson, Comprehensive Inorganic Chemistry; Pergamon Press, 1975, Vol III, 517.
15. G. Shiran, D.E. Cox, S.L. Ruby, *Phys. Rev* 125 (1962) 1158.
16. A. W. Coats, J. P. Redfern, *Nature* 68 (1964) 201.
17. B. K. Singh, R. K. Sharma, B. S. Garg, *Spectrochim. Acta A* 63 (2006) 96.
18. G. Longworth, B. Window, *J. Physics D* 4 (6) (1971) 835.
19. D.A. Scherson, S.B. Yao, E.B. Yeager, J. Eldridge, M.E. Kordesch, R.W. Hoffman, *J. Electroanalytical Chem. Interf. Electrochem.*, 150(1–2) (1983) 535.